Available online at www.sciencedirect.com
SCIENCE DIRECT®
Acta Materialia 52 (2004) 887–898
Acta MATERIALIA
www.actamat-journals.com

Wetting and reaction of MgO single crystals by molten Al at 1073–1473 K

Ping Shen *, Hidetoshi Fujii, Taihei Matsumoto, Kiyoshi Nogi

Joining and Welding Research Institute, Osaka University, 11-1 Mihogaoka, Ibaraki, Osaka 567-0047, Japan

Received 3 September 2003; received in revised form 3 September 2003; accepted 18 October 2003

Abstract

The wetting and reaction of molten Al on three different faces of MgO single crystals, (1 0 0), (1 1 0) and (1 1 1), at 1073–1473 K in a reduced Ar–3% H_2 atmosphere were investigated using an improved sessile drop method. The wettability depends significantly on neither the substrate orientation nor the temperature under the aforementioned conditions. The intrinsic contact angles are possibly between 90° and 105°. The reaction layer depth does not considerably vary with the MgO substrate orientation as well. The final reaction products are primarily α-Al_2O_3 phase for (1 0 0)MgO and κ′-, κ- and δ-Al_2O_3 phases for (1 1 0) and (1 1 1)MgO, without a pronounced $MgAl_2O_4$ phase. The reactive wetting kinetics is characterized by three representative stages. The reasons for the weak dependence of the wettability on the MgO substrate crystallographic orientation and the effect of the reaction on the wetting are presented.

Keywords: Wettability; Surface and interface; Substrate orientation; Reaction; Kinetics

1. Introduction

A comprehensive understanding of the wettability of ceramics by liquid metals as well as the influencing factors is not only of scientific interest but also of significant technological importance for a variety of applications such as composite fabrication, thin film deposition and joining. It has been realized that the wettability is not only determined by the thermodynamic characteristics of the metal–ceramic system such as solubility and reactivity, but also by some external factors such as working atmosphere (especially oxygen partial pressure), impurities and substrate surface conditions including surface roughness, crystallographic orientation, adsorption, etc. [1], and an established method for studying these factors is to investigate the behavior of a molten metal sessile drop on a ceramic substrate under different physical conditions [2].

The wetting of molten Al on MgO substrates has been investigated by several researchers. For instance, Mcevoy et al. [3] studied the wetting of the Al–(1 0 0)MgO system in a vacuum at temperatures between 1000 and 1350 K and found that the equilibrium contact angle could not be measured and the systematic observation of the contact angle variation was of little significance due to an extensive chemical reaction between the molten Al and the (1 0 0)MgO substrate. They indicated that the primary reaction product in the reaction zone was spinel ($MgAl_2O_4$) with a fixed Mg/Al ratio, while at the reacted substrate surface, the presence of an Al_2O_3 phase with a small trace of Mg was also observed. The growth of the spinel layer in the depth profile was argued to be controlled by the reaction, not by diffusion of the Al and Mg species through the spinel phase. Similar reaction products at the Al–(1 0 0)MgO interface were also identified by Weirauch [4], who studied the interfacial phenomena between the (1 0 0) periclase single crystals and pure Al as well as an Al–3 wt% Mg alloy at 1073 K in both a flowing argon atmosphere and a medium vacuum. He argued that the formation of the Al_2O_3 phase at the reacted periclase surface was due to the supply of the magnesium from the reaction front failing to compete with its loss through volatilization.

* Corresponding author. Tel./fax: +81-6-6879-8663.
E-mail address: shenping@jwri.osaka-u.ac.jp (P. Shen).

1359-6454/$30.00 © 2003 Acta Materialia Inc. Published by Elsevier Ltd. All rights reserved.
doi:10.1016/j.actamat.2003.10.024

The contact angles were reported as 135° and 90° for pure Al and the Al–3 wt% Mg alloy, respectively, after a dwelling time of 100 min. In contrast, one of the authors (Fujii [5–7]), in a previous study, found that the reaction products were sensitive to the type of the MgO substrate, i.e., whether a single crystal or a polycrystal was used. The primary reaction product at the Al–(1 0 0)MgO interface was α-Al_2O_3 while that at the Al–polycrystalline MgO interface was the spinel phase(s) ($MgO \cdot Al_2O_3$ or/and $CaO \cdot Al_2O_3$, depending on the initial impurity in the polycrystals). On the other hand, the wetting progress in the Al–MgO system was characterized by four dynamic stages [8] and a criterion for evaluation of the true wetting improvement in systems with a significant volume loss during the wetting process was put forward [6,7].

Despite these studies, the intrinsic wettability of the MgO substrates by the molten Al has not yet been determined. The main difficulty may lie in the influences of the molten Al surface oxidation at relatively low temperatures and the chemical reaction between Al and MgO at relatively high temperatures. The reaction products, especially those in the MgO single crystals, are also still in dispute, and their formation mechanisms are not very clear. Additionally, the effect of the MgO substrate orientation on the wettability in this system, to the best of our knowledge, has never been experimentally investigated even though it is an important question, particularly in crystal/film epitaxial growth and adhesion. A comparative study concerned with the effect of the MgO substrate orientation on the wettability was performed by one of the authors (Nogi [9]) in non-reactive Me(Me = Pb, Sn and Bi)/MgO systems using the (1 0 0), (1 1 0) and (1 1 1) faces of MgO single crystals at 873 K in a purified hydrogen atmosphere. It was found that the wettability was essentially dependent on the MgO substrate orientation as well as heat treatment of the substrate surface. The wettability and adhesion are in the order of (1 0 0) > (1 1 1) > (1 1 0). This dependency was interpreted by a simple model considering the affinity between the top-layer oxygen atoms and the neighboring liquid metal atoms at the solid–liquid interface along with the influence of the coulomb force between the top-layer oxygen ions and the second-layer Mg ions at the MgO surfaces.

The objective of this study was to investigate the wettability of the MgO single crystals by molten Al at temperatures between 1073 and 1473 K with a particular interest in the effect of the MgO substrate orientation as well as the effect of the interfacial reaction on the wetting behavior.

2. Experimental procedure

Pure Al (> 99.99 wt%) and pure MgO single crystals (Nakazumi Crystal Laboratory Co. Ltd., Japan) were used as the raw materials. Small Al segments weighing about 0.1–0.15 g were cut from a 3-mm diameter Al wire. The MgO single crystal wafers with dimensions of 20 mm × 20 mm × 0.5 mm were cut along (1 0 0), (1 1 0) and (1 1 1) crystallographic planes with an orientation error of ±0.5°. One side of these surfaces was polished to an average roughness of 200 Å (20 nm) (measured by a DEKTAK 3 Surface Profilometer, Japan). Before the experiment, both the MgO wafer and the Al segment were carefully cleaned in acetone using an ultrasonic machine.

An improved sessile drop method [10] was employed in this study and the experiments were conducted in a stainless-steel chamber, using a tantalum cylindrical heater shielded by five-layer concentric Mo reflectors. The experimental apparatus also consists of an evacuating system with a rotary pump and a turbo molecular pump (TMP), a gas purification system, a dropping device, a temperature program controller using a W-5% Ra/W-26% Rh thermocouple, a 10 mW He–Ne laser, a band-pass filter, a high-resolution (2000 × 1312 pixels) digital camera with a remote controller, a video and an image automatic transmission and processing system. The band-pass filter can cut all other wavelengths except for the laser beam (632 nm). As a result, the reflection light inside the chamber at high temperatures can be removed and high definition drop profiles can be obtained.

After the MgO wafer was set in a horizontal position on an Al_2O_3 supporter inside the chamber and the Al segment was placed in a glass tube with a spring connector on the top of the dropping device outside the chamber (a schematic diagram was given in Ref. [10]), the chamber was evacuated to about 5×10^{-4} Pa and then heated to the desired temperature in vacuum at the heating rate of 20 °C/min. For the experiments performed at temperatures lower than 1373 K, the temperature was first raised to 1373 K, maintained for 10 min and then cooled to the desired experimental temperature. Such a procedure was to remove substrate surface contaminants as well as to obtain a higher vacuum. The chamber was then purged with a premixed Ar–3% H_2 gas purified using platinum asbestos and magnesium perchlorate and the pressure was controlled to about 120 kPa (approx. 1.2 atm). The oxygen partial pressure was estimated to be less than 10^{-14} Pa [11]. After the temperature and the atmosphere had stabilized, the Al segment was inserted into the bottom of the alumina tube and kept for 1 min in order for it to melt and reach the experimental temperature. The molten Al was then forced out from a small hole ($\varnothing = 1$ mm) in the bottom of the alumina tube and dropped onto the MgO substrate by a gradual decrease in the pressure inside the chamber to about 110 kPa (approx. 1.1 atm). At the same time, the initial oxide on the Al surface was mechanically removed as the liquid passed through the small hole.

To avoid the droplet impact with the substrate and thus producing a receding contact angle [12], the dropping distance was controlled to no more than 4 mm, at which the droplet could contact both the substrate and the bottom of the Al_2O_3 dropping tube when it fell from the small hole. The Al_2O_3 supporter stage was then slowly and slightly lowered to let the droplet break away from the Al_2O_3 dropping tube. As soon as the droplet separated from the dropping tube, a photo was taken and defined as the drop profile at zero time. Subsequent photos were taken at specific time intervals. The captured photographs were analyzed using an axisymmetric-drop-shape-analysis (ADSA) program, by which the contact angle, surface tension and density could be simultaneously calculated. This program offers a high degree of accuracy while being free of the operator's subjectivity.

Generally, two runs of the experiments were performed at every experimental temperature, however, if the contact angles measured in the two runs differed more than a few degrees, the third or more repeated experiments were conducted.

After the wetting experiments, some samples were vertically sectioned to prepare the metallographic specimens and some were etched in a 15 wt% NaOH distilled-water solution to remove the Al droplet. The latter treatment allows the measurement of the surface topography using a DEKTAK 3 surface profilometer. Microstructures were observed by a laser 3D profile microscope (Keyence, VK-8550, Japan) and an environmental scanning electron microscope (ESEM-2700, Nikon Co., Japan), and the reaction phases were identified by EDAX and X-ray diffraction (XRD).

3. Results

3.1. Contact angle phenomena

Figs. 1–5 show the variations in contact angles of the molten Al on the three faces of MgO single crystals at temperatures between 1073 and 1473 K as plotted on a logarithmic timescale. As can be seen, at low temperatures (up to $T = 1273$ K), the contact angle does no considerably vary with time during the isothermal dwellings. However, at high temperatures ($T > 1273$ K), a noticeable decrease in the contact angle with time is observed. The initial contact angles, typically at times less than 60 s, do not show a significant difference in the above temperature range and are generally between 90° and 105°, except for those at 1073 K, which are much higher and possibly affected by the molten Al surface oxidation. More importantly, the initial contact angles, on the whole, do not show a *remarkable* and *constant* dependence on the MgO substrate orientation. On the other hand, they exhibit a relatively larger scatter in the

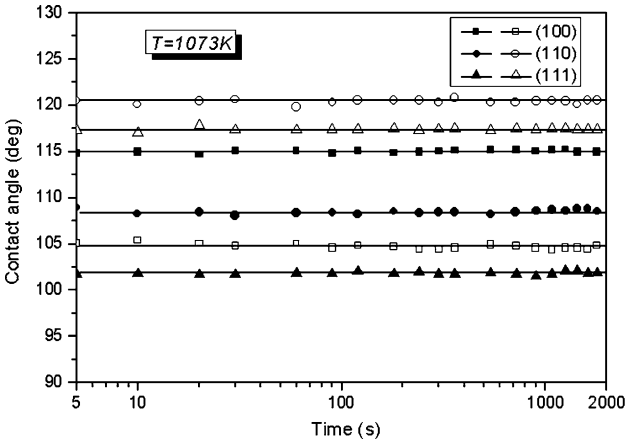

Fig. 1. Variation in contact angle with time for molten Al on three faces of MgO single crystals during dwelling at 1073 K as plotted on a logarithmic timescale.

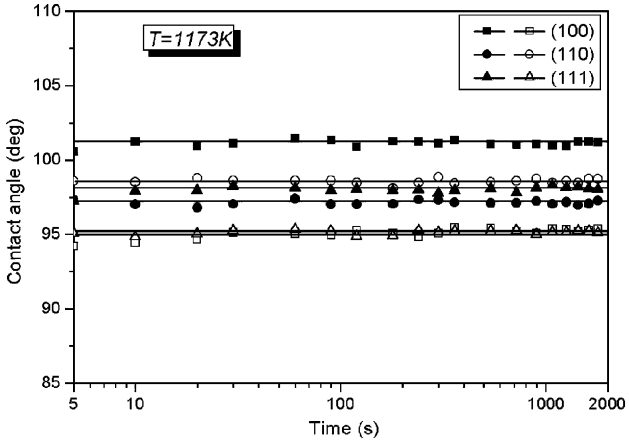

Fig. 2. Variation in contact angle with time for molten Al on three faces of MgO single crystals during dwelling at 1173 K as plotted on a logarithmic timescale.

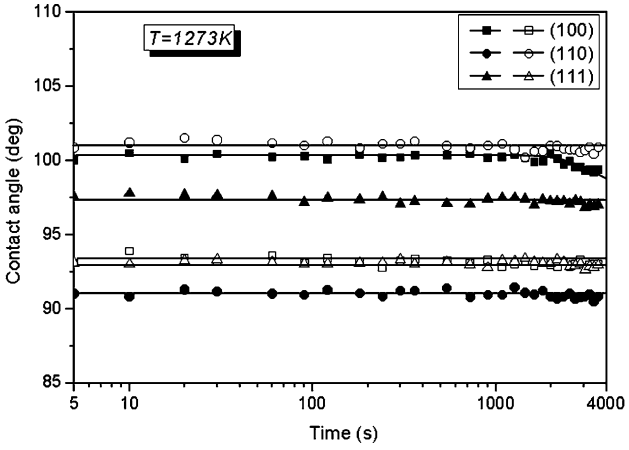

Fig. 3. Variation in contact angle with time for molten Al on three faces of MgO single crystals during dwelling at 1273 K as plotted on a logarithmic timescale.

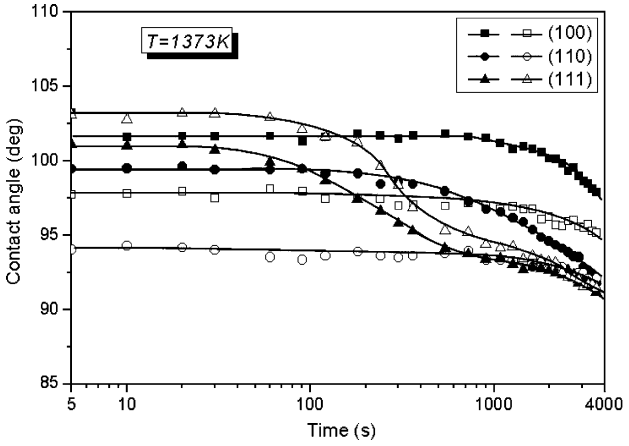

Fig. 4. Variation in contact angle with time for molten Al on three faces of MgO single crystals during dwelling at 1373 K as plotted on a logarithmic timescale.

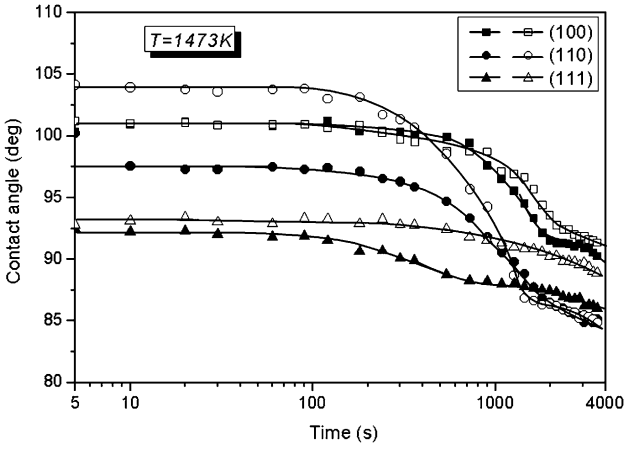

Fig. 5. Variation in contact angle with time for molten Al on three faces of MgO single crystals during dwelling at 1473 K as plotted on a logarithmic timescale.

different runs of the experiments as compared to other systems such as Al/α-Al_2O_3 under the same experimental conditions [10], which may mask this weak dependence if it really presents.

Fig. 6 shows the effect of MgO substrate annealing on the wettability of this system at 1173 K. It seems that the high temperature annealing does not have a significant effect on the wettability if the experimental scatter is taken into account, or alternatively, it may slightly weaken the wettability due to the MgO surface faceting [13–16] and/or reconstruction [17,18] during the annealing process, which decrease their surface free energies. This result is essentially different from that in the non-reactive Me (Me = Pb, Sn and Bi)/MgO systems at 873 K [9], in which the wettability was found to be promoted by annealing the MgO substrates at 1400 K for 3600 s.

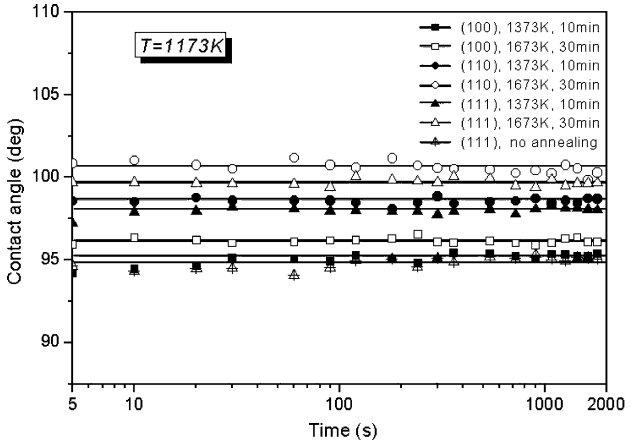

Fig. 6. Effect of substrate annealing on the wettability of the Al–MgO system at 1173 K.

3.2. Interfacial reaction and reaction products

Microstructural observations indicate that the interfacial reaction occurred in all the Al–MgO samples after experiments at the temperatures higher than 1073 K. The reaction zone, typically characterized by the reaction layer length and depth [5], increases with both the temperature and time. A representative reaction zone profile of an Al–(1 1 0)MgO sample is illustrated in Fig. 7. Note that the reaction zone extended out of the triple junction and the reaction layer length was larger than the depth after dwelling at 1473 K for 3600 s, indicating that the reaction proceeded more easily in the horizontal-surface direction than that in the vertical-depth direction. However, the reaction layer length at the periphery of the Al droplet differs relatively largely at different surface directions, as indicated in Fig. 7(b), therefore, only the reaction layer depth was used here to characterize the reaction extent. Table 1 shows the reaction layer depths in the Al–MgO samples after dwelling at 1273–1473 K for 3600 s. As can be seen, the reaction layer depths are quite similar, without a significant dependence on the substrate orientation, except for that of the (1 0 0) face being slightly smaller at 1273 K.

The EDAX and XRD analyses indicate that the reaction products in all the reacted samples are mainly Al_2O_3 phases, without a pronounced spinel ($MgAl_2O_4$) phase. The Mg and Al species at the MgO–Al_2O_3 interface, both in a vertical depth profile (see Fig. 8(a)) and a horizontal surface profile (see Fig. 8(b)), vary rather sharply. However, in places where a transition phase is present (see Fig. 9), the Mg and Al compositional alterations are not so drastic, implying that the reaction progress and the growth of the reaction layer might be still partly controlled by diffusion of the Mg and Al atoms through the transition phase, which, as demonstrated by the EDAX analysis, does not

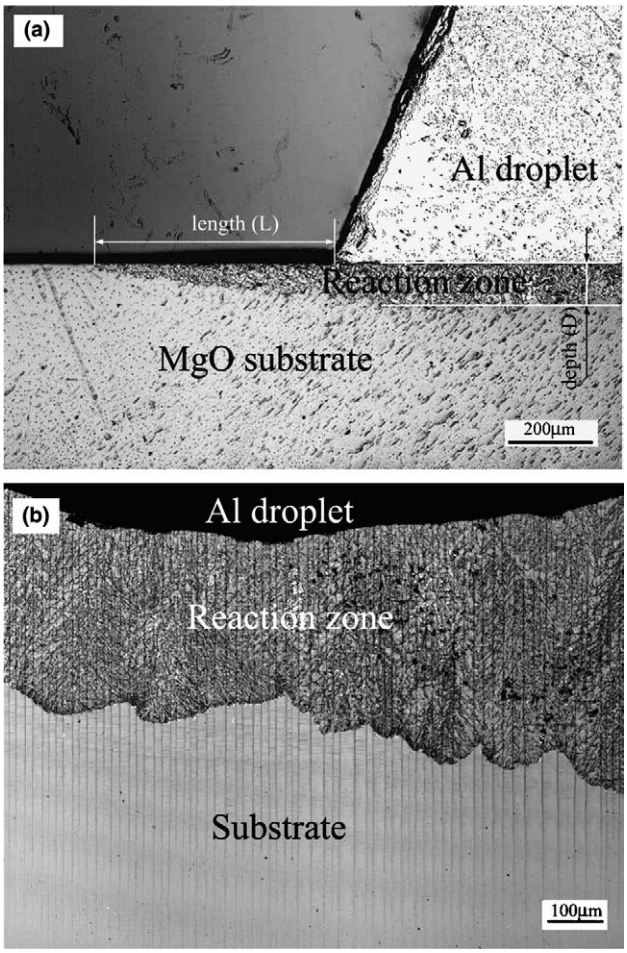

Fig. 7. A reaction zone in a vertical-depth profile (a) and a horizontal-surface profile (b) of an Al–(1 1 0)MgO sample after dwelling at 1473 K for 3600 s.

Table 1
Reaction layer depths in the Al–MgO samples after dwelling at 1073–1473 K for 3600 s

System	Reaction layer depth (μm)		
	1273 K[a]	1373 K	1473 K
Al–(1 0 0)MgO	42	70	112
Al–(1 1 0)MgO	49	73	112
Al–(1 1 1)MgO	50	71	115

[a] The values at 1273 K are the maximum depths of the separated reaction layers beneath the reacted MgO surface.

correspond to the $MgAl_2O_4$ phase but to a Mg–Al–O compound (see Table 2). The sharp elemental alteration at the MgO–Al_2O_3 interface is thought to be a result of Mg rapid evaporation either directly from the reacted surface/interface or through the liquid Al after it was displaced from the MgO substrate or the transition phase. In fact, fine Mg powders were found deposited on the chamber wall after every high-temperature experiment.

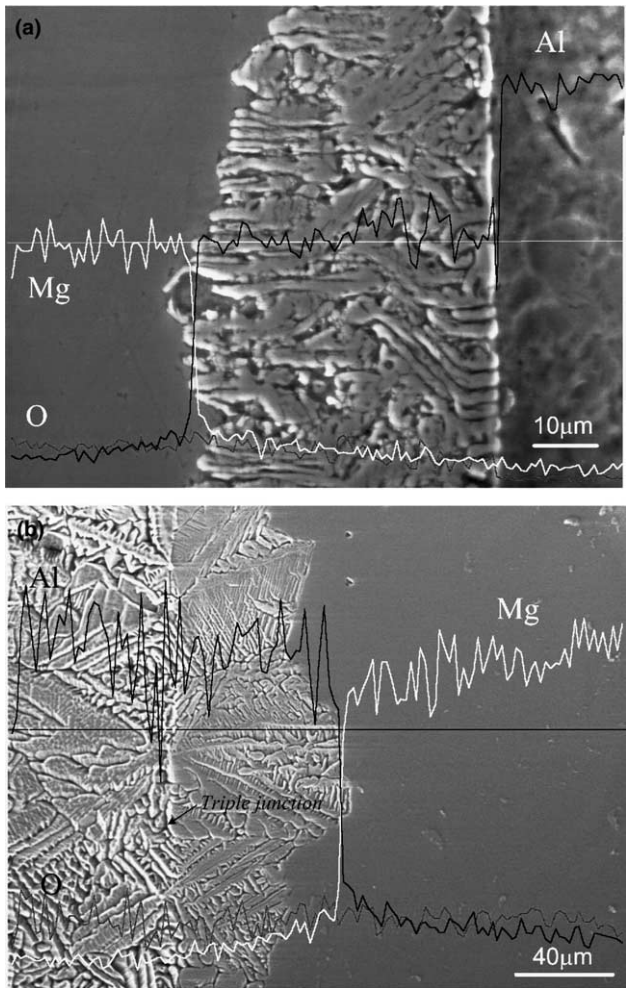

Fig. 8. Microstructures and elemental composition alternations at a vertical-section interface (a) and a horizontal triple-junction interface (b) (after removal of the Al droplet) in an Al–(1 1 1)MgO sample after dwelling at 1273 K for 3600 s.

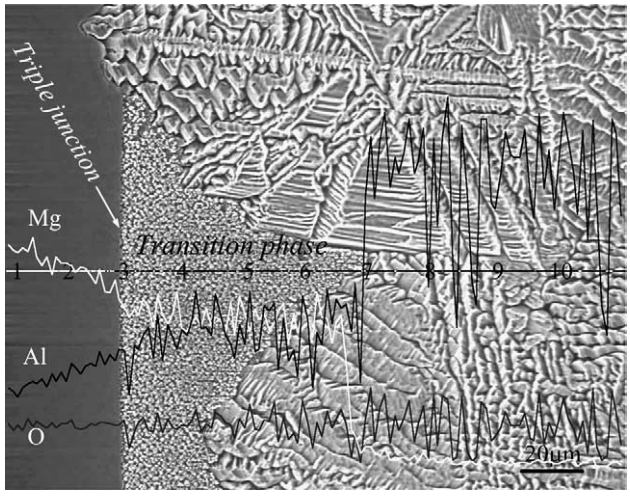

Fig. 9. Composition alternations of the Al, Mg and O elements at a triple junction with a transition phase in an Al–(1 0 0)MgO sample after dwelling at 1273 K for 3600 s. Detailed compositions of the Al and Mg species at the labelled points are given in Table 2.

Table 2
Mg, Al atomic compositions of the points labelled in Fig. 9

Element	Atomic composition (at.%)									
	1	2	3	4	5	6	7	8	9	10
Mg	60.50	59.37	47.97	42.60	41.34	42.17	22.51	7.59	5.84	5.16
Al	39.50	40.63	52.03	57.40	58.66	57.83	77.49	92.41	94.16	94.84

On the other hand, the XRD results reveal that the formed Al_2O_3 products are sensitive to the substrate orientation. Figs. 10–12, respectively, show the XRD spectra of the Al–(1 0 0), (1 1 0) and (1 1 1)MgO interfacial (and surface) phases after removal of the solidified Al droplet as compared to those of the as-received and annealed MgO surfaces. Clearly, the primary reaction product at the Al–(1 0 0)MgO interface is α-Al_2O_3 while that at the Al–(1 1 0)MgO and Al–(1 1 1)MgO interfaces is κ'-, κ-, and δ-Al_2O_3 phases. The latter phases are usually obtained during the dehydration of the hydrated α-Al_2O_3 phase [19,20], therefore, it was first conjectured that the H_2 atmosphere employed in the experiments was responsible for their formation. However, our later experiments under purified Ar atmosphere (>99.999% purity) demonstrate that the same reaction products were produced at the Al–(1 1 0) and (1 1 1)MgO interfaces. As a result, the H_2 atmosphere should not be the decisive factor. The true reasons for their formation remain unclear at the present time.

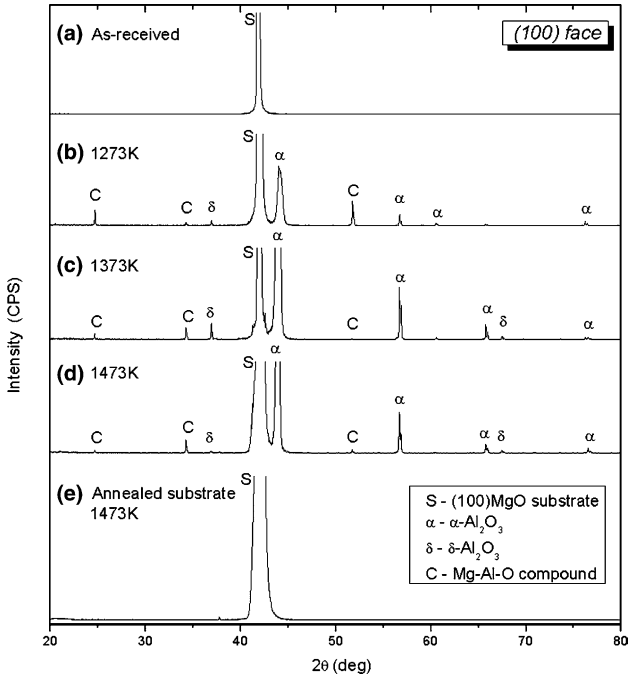

Fig. 10. XRD spectra of the interfacial (and surface) phases in the Al–(1 0 0)MgO samples after removal of the solidified Al droplet as compared to the as-received (unheated) and annealed (1 0 0)MgO specimens. (Some strong peaks of the major phases are cut in order to show all the minor phases.)

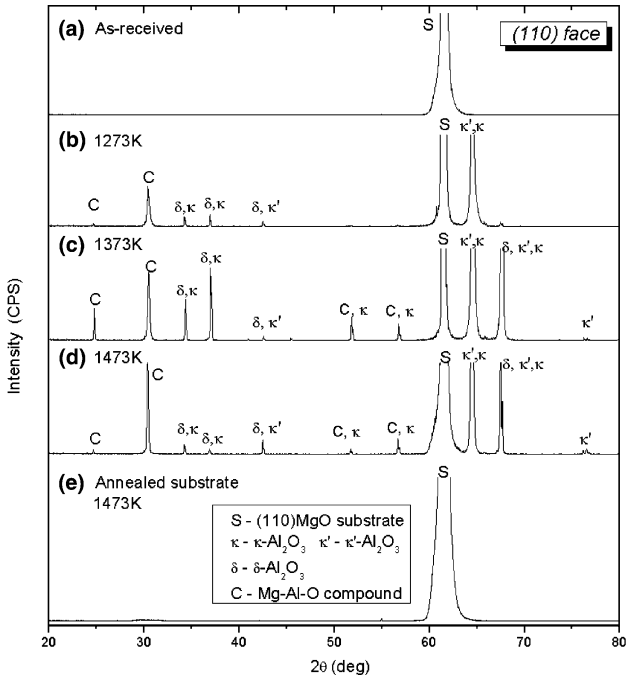

Fig. 11. XRD spectra of the interfacial (and surface) phases in the Al–(1 1 0)MgO samples after removal of the solidified Al droplet as compared to the as-received (unheated) and annealed (1 1 0)MgO specimens. (Some strong peaks of the major phases are cut in order to show all the minor phases.)

4. Discussion

4.1. Possible intrinsic contact angles of the Al–MgO system

In a reactive wetting system, wetting is usually coupled with reaction and the contact angle progressively decreases as the reaction proceeds, especially during the initial reaction period. Consequently, the intrinsic contact angle of the original system might either fail to be detected or wrongly characterized. As mentioned earlier, Mcevoy et al. [3] argued that the equilibrium contact angle of the Al–(1 0 0)MgO system could not be obtained and their systematic observation of the contact angle variation was of little significance in establishing the adhesion of the Al–MgO system because of the change in interfacial phases as well as the lack of a steady equilibrium state. In fact, the intrinsic wettability of a reactive system, particularly for a strong reaction system, cannot be accurately determined without using

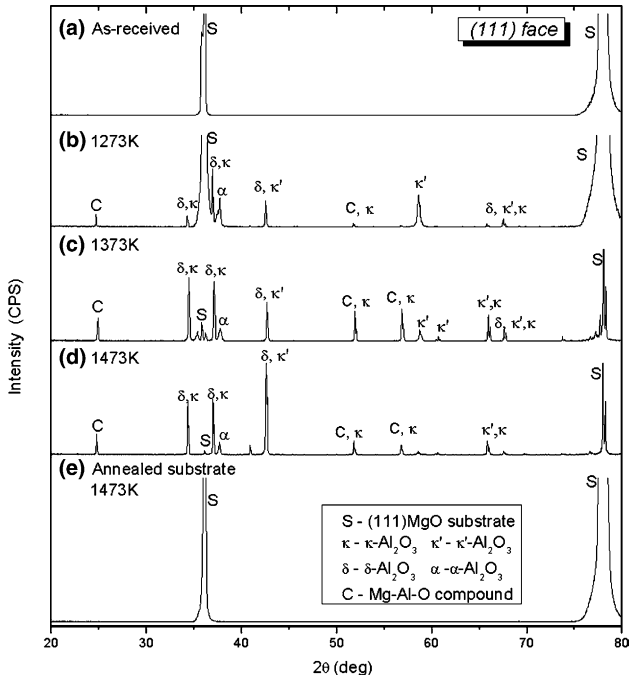

Fig. 12. XRD spectra of the interfacial (and surface) phases in the Al–(1 1 1)MgO samples after removal of the solidified Al droplet as compared to the as-received (unheated) and annealed (1 1 1)MgO specimens. (Some strong peaks of the major phases are cut in order to show all the minor phases.)

an improved sessile drop method and an instantaneous drop-profile recording technique [12].

In our experiments, as presented in Figs. 1–5, the contact angles of the Al–MgO system at low temperatures do not significantly vary with time during the isothermal dwellings, while those at high temperatures progressively decrease with time. The decrease obviously results from the interfacial reaction between Al and MgO, which changes the interface/surface conditions either by release of the reaction energy [21] or by change in the interfacial chemistry at the triple junction [22], and those contact angles, in nature, no longer represent the original Al–MgO system. In contrast, the initial contact angles, which remain almost constant, typically at times between 10 and 30 s, might be the intrinsic ones of the Al–MgO system if they are not significantly affected by the molten Al surface oxidation and/or H_2 adsorption on the MgO surfaces. For a clear comparison, Table 3 lists the values of the contact angles at 30 s (θ_{30}) in the Al–MgO samples as presented in Figs. 1–5. It seems that they depend strongly on neither the temperature nor the substrate orientation. The contact angles at 1073 K are much larger and more scatter as compared to those at higher temperatures, which is mainly attributed to the Al surface oxidation. A prior Al–Al_2O_3 wetting study under the same experimental conditions indicated that the Al surface oxidation could not be completely avoided at $T < 1223$ K, however, at $T = 1173$ K, the effect was minor and at $T > 1223$ K, the effect was negligible [12]. In this context, the relatively large scatter in the contact angles as well as some abnormally large values at high temperatures may not be wholly attributed to the Al surface oxidation, other factors such as H_2 adsorption [23–32], MgO surface faceting [13–16] and/or reconstruction [17,18] may also account for them.

4.2. Explanation for the weak dependence of the wettability on the MgO substrate orientation

The result of the weak dependence of the Al–MgO wettability on the MgO substrate orientation seems somewhat unexpected. As in the previous study on the non-reactive Me (Me = Pb, Sn and Bi)/MgO systems at 873 K in a purified H_2 atmosphere [9], the wettability was found essentially dependent on the MgO substrate orientation which is in the order of (1 0 0) > (1 1 1) > (1 1 0). On the other hand, theoretical studies of the transition metals, such as Pd, Cu and Ag, deposition on the MgO substrates [33–36] indicated that the work of adhesion on the (1 1 0) and (1 1 1) surfaces was much stronger than that on the neutral (001)MgO surface, i.e., the wettability of the former two was better than that of the latter as deduced from the Young-Dupré equation

$$W_{ad} = \sigma_{lv}(1 + \cos\theta), \quad (1)$$

where W_{ad} is the work of adhesion and σ_{lv} is the liquid–vapor interfacial free energy.

The exact reasons for the different results in the aforementioned metal–MgO systems are unclear, however, as far as the Al–MgO system is concerned, the following factors are noteworthy which may explain the results obtained in this study:

First, although the (1 1 1)MgO surface is polar and known as energetically unstable as compared to the (1 0 0) surface [37], and the surface free energies of the three faces at ambient temperature are in the order of

Table 3
The contact angles at 30 s (θ_{30}) for molten Al on the three faces of MgO substrates at various temperatures as presented in Figs. 1–5

System	Contact angles at 30 s, θ_{30} (deg.)				
	1073 K	1173 K	1273 K	1373 K	1473 K
Al–(1 0 0)MgO	110 ± 5	98 ± 3	96 ± 4	99 ± 2	101
Al–(1 1 0)MgO	114 ± 6	98 ± 1	96 ± 5	97 ± 3	100 ± 3
Al–(1 1 1)MgO	110 ± 8	96 ± 2	95 ± 3	102 ± 1	93 ± 1

(1 1 1) > (1 1 0) > (1 0 0) [38–41], a number of experimental and theoretical studies support the main idea that the (1 1 0) and (1 1 1)MgO surfaces spontaneously facet into the (1 0 0) (or other low-energy) face(s) in a microscopic size [13–16], and/or reconstruct [17,18] in order to lower their relatively high surface free energies during annealing. The surface faceting, as observed by Henrich [13] and Chern et al. [14], can occur even after annealing the substrate at 900 K. At higher temperatures, the faceted scale is greater than a few micrometers [13,14] and the surface reconstruction is distinguishable [16,18]. The reconstruction, on the other hand, can also be driven by desorbed hydroxyl group after annealing the substrates at low temperatures as observed on a polar (1 1 1)NiO surface [42], which is similar to MgO in crystal structure. Accordingly, the weak effect of the high temperature annealing on the wettability (as indicated in Fig. 6), to a certain extent, might be attributed to the initiation of surface faceting at low temperatures, while the relatively large scatter in the measured contact angles might be explained by an increase in surface roughness induced by a significant surface faceting and/or reconstruction.

Second, as demonstrated by theoretical density functional calculations [43], the bonds at the Al/oxygen-terminated (1 0 0)MgO interface are much stronger than those at the Al/magnesium-terminated (1 0 0)MgO interface. Therefore, the adhesion and the wettability are primarily determined by the quantity, or more exactly, the density of the oxygen atoms at the top-layer of the MgO surfaces, which is very similar to that found in the Al/α-Al_2O_3 system as we have described in detail in Ref. [44]. In addition, theoretical calculations and experimental observations both favor that the geometry of the MgO surfaces can be characterized by surface rumples with the Mg atoms moving inwards and the oxygen atoms moving outwards [40,41]. Atomic force microscope (AFM) observation on the MgO surfaces further provides the images of the MgO surface structures, which are quite different from the bulk ones [45]. Fig. 13 shows schematic diagrams of different oriented MgO surface and bulk structures, from which the number of the oxygen atoms both at the surface and in the bulk can be calculated and the results are presented in Table 4. Apparently, the densities of the oxygen atoms at the three surfaces are not very different, implying similar Al–O bonds at the Al–MgO interfaces and hence the similar adhesion and wettability of the different oriented MgO substrates by molten Al.

Finally, the H_2 atmosphere employed in the experiments might also have an influence on the wettability. Fig. 14 compares the contact angles in the Al–(1 1 1)MgO samples at 1373 K under the purified Ar–3% H_2 and pure Ar atmospheres. As can be seen, the initial contact angles under the Ar atmosphere are a few degrees smaller than those under the Ar–3% H_2 atmosphere. Similar results were also obtained in the Al–(1 1 0)MgO samples. However, due to the relatively large scatter of the contact angles in the Al–MgO system as

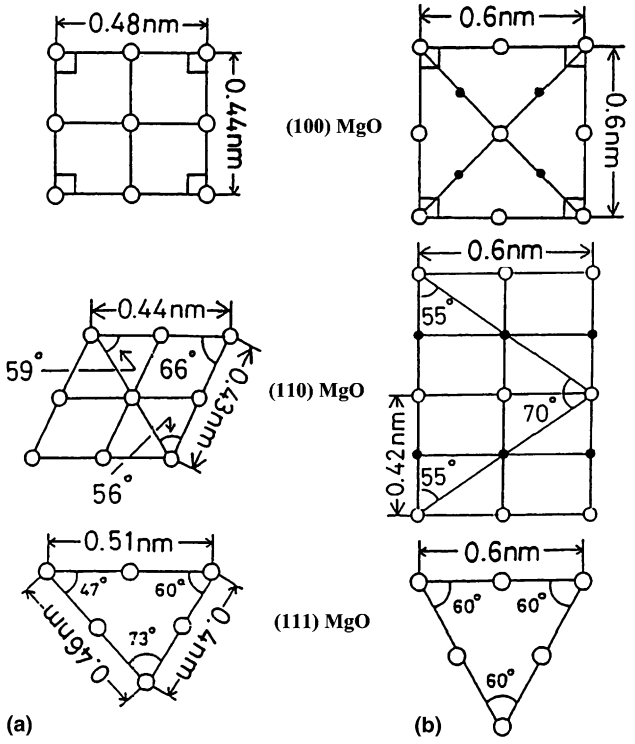

Fig. 13. Schematic diagrams of the (1 0 0), (1 1 0), (1 1 1)MgO surface structures (a) and bulk structures (b) [45].

Table 4
Number of oxygen atoms at the MgO surfaces and in the bulk crystals

Crystal	Number of oxygen atom ($\times 10^{-5}$ mol m^{-2})	
	Surface	Bulk
(1 0 0)	3.15	1.85
(1 1 0)	3.85	1.32
(1 1 1)	3.87	2.13

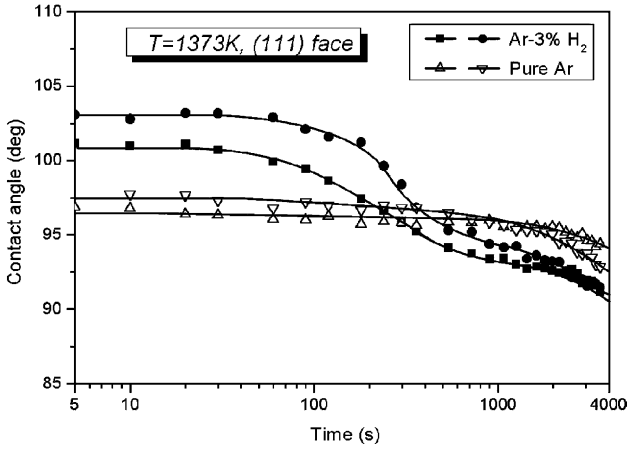

Fig. 14. Comparison of the contact angles in the Al–(1 1 1)MgO samples at 1373 K under the Ar–3% H_2 and pure Ar atmospheres.

well as the relatively minor difference in the results under these two atmospheres conditions, we are not very certain to draw the conclusion of the influence of H_2 and its extent. It is numerously reported that H_2 can adsorb on and further interact with the MgO surfaces [23–32]. Ab initio total-energy calculations performed by Refson et al. [46] showed that a chemisorption reaction involving a reconstruction to form a (1 1 1) hydroxyl MgO surface was strongly preferred. They even claimed that the protonation stabilized the otherwise unstable (1 1 1) surface and that this, not the neutral (1 0 0), was the most stable MgO surface under ambient conditions. The hydroxylation is regarded as a particularly efficient mechanism for stabilization of the (1 1 0) and (1 1 1)MgO surfaces since it decreases their surface energies. However, considering that dehydroxylation usually occurs at temperatures higher than 1073 K, the function of H_2 may be limited since the gas was introduced after the experimental temperature was reached. Nevertheless, there are also reports that the faceted (1 1 1)MgO surface has a higher absorptivity and reactivity [47] and the binding energy of water on an Al-doped (1 0 0)MgO surface is much higher that that on the pure (1 0 0)MgO surface [48]. Therefore, if the H_2 molecules could indeed adsorb on and interact with the MgO surfaces at high temperatures, the differences in the surface free energies of the three faces would be reduced.

4.3. Wetting kinetics

Fig. 15 shows an example of the variations in contact angle and droplet characteristic size (base diameter, D and height, H) with time in an Al–(1 0 0)MgO sample during dwelling at 1473 K as plotted on a linear timescale (a) and a logarithmic timescale (b). Similar wetting behaviors were also observed in the Al–(1 1 0)MgO and Al–(1 1 1)MgO samples. As suggested by Fujii et al., the wetting kinetics can be characterized by the following stages: (I) an initial rapid spreading stage, (II) a quasi-equilibrium stage and (III) a chemical-reaction-wetting stage [6–8]. The wetting (or spreading) in stage (I) is driven by mechanical force for balancing the interfacial free energies as described by Young's equation. Typically, this stage is very short and is essentially similar to that in an inert system, which usually finishes in less than 1 s after the droplet contacts the substrate [8]. However, in our experiments, it takes several seconds due to the droplet vibration after its breakaway from the dropping tube. The wetting in stage (II) can be regarded as in a quasi-equilibrium state since the contact angle and droplet characteristic size remain almost constant. No interfacial reaction has occurred or yet substantially affected the wetting equilibrium. The contact angle in this stage, as we have indicated, may represent the intrinsic wettability of the Al–MgO system if they are not experimentally influenced. The duration of this stage dramatically decreases with temperature. For instance, it takes more than 2000 s at 1273 K while less than 720 and 180 s at 1373 and 1473 K, respectively, as in the Al–(1 0 0)MgO samples. In stage (III), the contact angle and droplet height continuously decrease as the reaction proceeds, whereas, the droplet base diameter first increases and then remains constant. In view of the different changes in the droplet base diameter, this stage can again be divided into an interfacial front (as well as the contact angle) advancing stage (labelled as III-a in Fig. 15) and the advancing stopping yet the contact angle continuously decreasing stage (labelled as III-b). Stage (III-a) is relatively shorter as compared to stage (III-b). An interfacial front receding stage, as previously described by Fujii and Nakae [8], however, was not observed in this study possibly due to the relatively short experimental time.

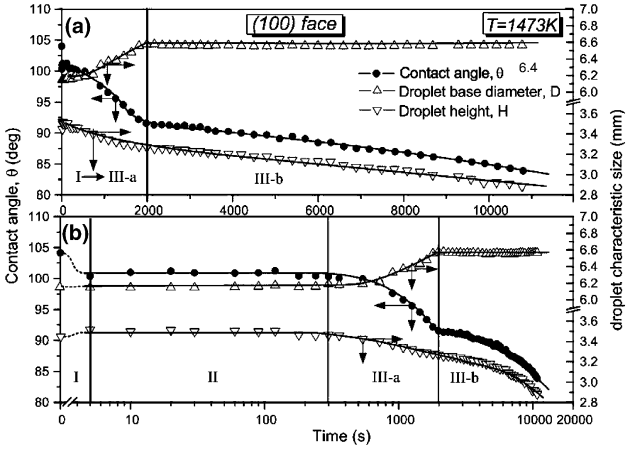

Fig. 15. Variations in contact angle and droplet characteristic size (base diameter and height) with time in an Al–(1 0 0)MgO sample during dwelling at 1473 K as plotted on a linear timescale (a) and a logarithmic timescale (b).

4.4. Effect of reaction on wetting

The advance of the interfacial front (i.e., the triple line) in stage (III-a) is essentially related to the interfacial reaction between the molten Al and MgO substrate. However, the interfacial reaction does not always lead the triple line to advance. A simple example is that the interfacial reaction between Al and all the MgO substrates at 1273 K is comparatively developed after 1800 s, especially at or near the triple junctions as illustrated in Fig. 16, however, the contact angle, as well as the droplet base diameter, does not show a noticeable decrease even after dwelling at that temperature for 3600 s except for a minor change displayed in one of the Al–(1 0 0)MgO samples as indicated in Fig. 3. Another example is that the interfacial reaction at higher temperatures continues

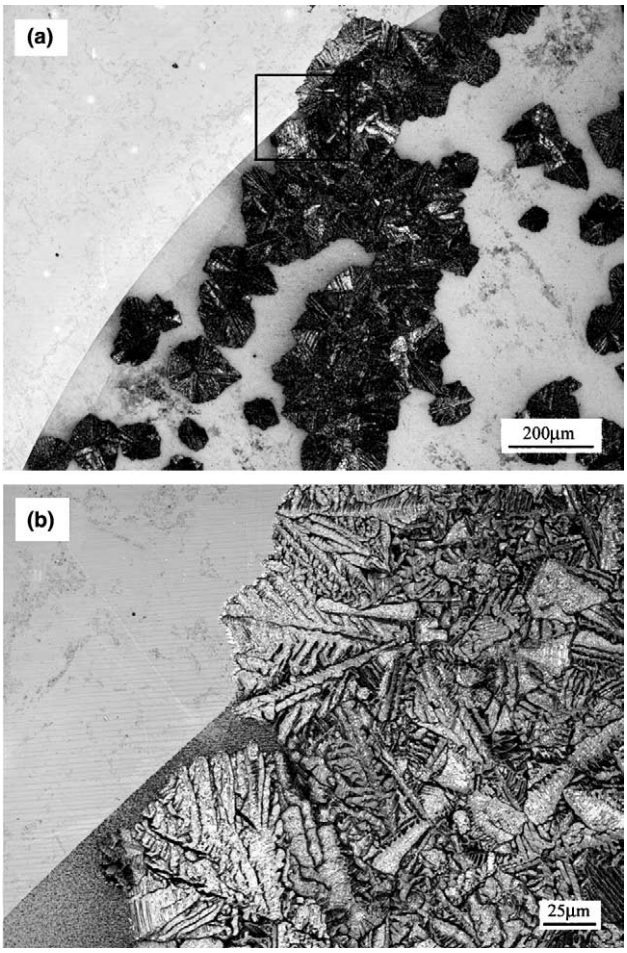

Fig. 16. Microstructures at and near the triple junction in an Al–(1 1 0)MgO sample dwelling at 1273 K for 1800 s after removal of the Al droplet. Image (b) shows the magnified microstructure of the frame area in image (a). EDAX analysis identified that the newly formed phases were Al_2O_3.

Table 5
The ultimate advancing contact angles, θ_{ad}, and the times when they reached, t_{ad}, at temperatures of 1373 and 1473 K

System	θ_{ad} (deg.)/t_{ad} (s)	
	1373 K	1473 K
Al–(1 0 0)MgO	97/4500	92/1800
	95/2520	93/1980
Al–(1 1 0)MgO	91/4200	88/1800
	93/3600	87/1800
Al–(1 1 1)MgO	93/1080	88/720
	92/1980	90/720

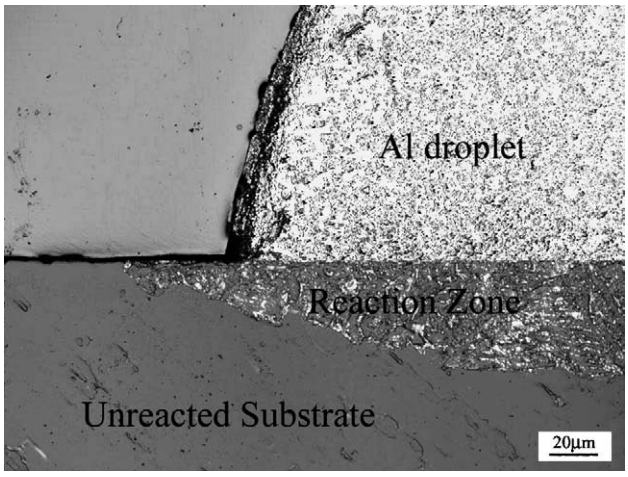

Fig. 17. A vertical-section interfacial microstructure in an Al–(1 1 0)MgO sample after dwelling at 1373 K for 1800 s, indicating that the interface has been transformed to an Al–Al_2O_3 rather than the original Al–MgO one at or before that time.

to progress yet the advance in the triple line stops after a certain time.

It is worthwhile to pay more attention to the ultimate advancing contact angles since they reflect the magnitude of the wetting enhancement by the chemical reaction and may be used for estimation of the equilibrium contact angle of the reacted system, as done by Fujii and Nakae [8]. Table 5 gives their values at 1373 and 1473 K together with the times when they reached. Note that the values are quite close in different runs of the experiments despite the relatively large scatter in the initial contact angles (see Figs. 4 and 5) and the difference in the times when they reached. Also, the contact angles of (1 1 0)MgO and (1 1 1)MgO are very close and they are slightly smaller than those of (1 0 0)MgO. It is reasonable to regard these contact angles as being from the reacted Al–Al_2O_3 system rather than the original Al–MgO system if one takes into account the interfacial structures at the times when they reached. Fig. 17 shows a vertical-section interfacial structure in an Al–(1 1 0)MgO sample after dwelling at 1373 K for 1800 s. As can be seen, the interface has been transformed to Al–Al_2O_3 rather than the original Al–MgO. On the other hand, the similar ultimate advancing contact angles in the (1 1 0)MgO and (1 1 1)MgO samples are possibly related to the similar Al_2O_3 phases (κ', κ and δ phases) formed at the solid–liquid interfaces while their difference from those of the (1 0 0)MgO samples is attributed to the different Al_2O_3 phases. Nevertheless, it should be borne in mind that these ultimate advancing contact angles are not the equilibrium ones for the Al–Al_2O_3 system because the wetting at the times when they reached is not in a chemical-equilibrium state [21]. The stop of the triple line advance, to a great extent, may be caused by an increase in the substrate surface roughness, particularly at the triple junctions, due to the MgO surface faceting, reconstruction, chemical reaction and subsequent formation of the Al_2O_3 products. Fig. 18 shows a surface profile in an Al–(1 1 0)MgO sample after dwelling at 1273 K for 1800 s, corresponding to the triple junction with a similar microstructure indicated in

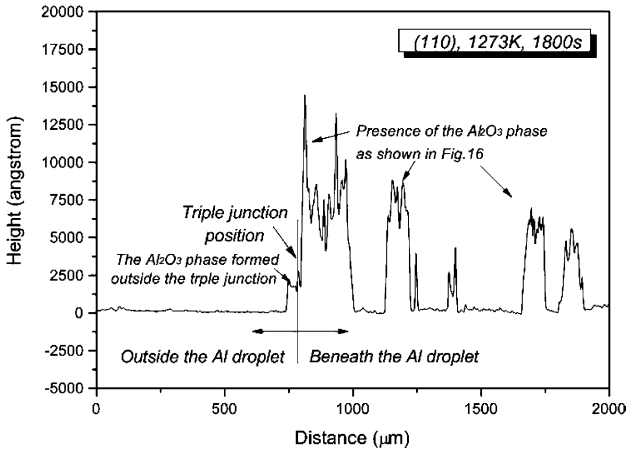

Fig. 18. Surface topography at the triple junction in an Al–(1 1 0)MgO sample after dwelling at 1273 K for 1800 s.

Fig. 16. Clearly, the surface topography at the triple junction is undulating, which can easily obstruct the advance of the triple line.

5. Summary and conclusions

The wetting and reaction of molten Al on three different oriented MgO single crystals, (1 0 0), (1 1 0) and (1 1 1), were investigated at 1073–1473 K mainly in a reduced Ar–3% H_2 atmosphere using an improved sessile drop method. The results show that the possible intrinsic contact angles in the Al–MgO system are between 90° and 105°, neither significantly depending on the substrate orientation nor on the temperature. The weak dependence of the wettability on the MgO surface orientation is explained by the similar densities of the oxygen atoms at the three MgO surfaces, the MgO surface faceting and reconstruction at high temperatures, and the H_2 molecules possible dissociative chemisorption on the MgO surfaces. The latter two are considered as favoring stabilization of the high energy (1 1 0) and (1 1 1) surfaces and thus alleviating the difference in the surface free energies among these three surfaces.

The reaction layer depth does not significantly vary with the MgO substrate orientation as well, although that in the (1 0 0)MgO samples appears to be slightly smaller at relatively low temperatures as compared to that in the (1 1 0) and (1 1 1)MgO samples. The final reaction products in the reaction zone are mainly Al_2O_3 phases, without a pronounced $MgAl_2O_4$ phase. However, the nature of the Al_2O_3 products is somewhat different. For (1 0 0)MgO, it is α-Al_2O_3, while for (1 0 0) and (1 1 1)MgO, it is κ′-, κ- and δ-Al_2O_3. The reasons for the formation of the different Al_2O_3 phases at the different faces of MgO surface (Al–MgO interface) are unclear at the present time.

The reactive wetting kinetics of the Al–MgO system is characterized by the following representative stages: (I) an initial rapid spreading stage, (II) a quasi-equilibrium stage and (III) a chemical-reaction-wetting stage. Stage (III) can be further divided into an interfacial front advancing stage (III-a) and an advancing stopping yet the contact angle continuous decreasing stage (III-b). The ultimate advancing contact angle represents the reacted Al–Al_2O_3 system rather than the original Al–MgO system. The advance in the triple line, i.e., the wetting enhancement, is essentially produced by the interfacial reaction, but on the other hand, the interfacial reaction does not always lead the triple line to advance. The increase in surface roughness, particularly at the triple junctions, can substantially drag the triple line from further advance.

Acknowledgements

This work is supported by the International Joint Research Grant Program from the New Energy and Industrial Technology Development Organization (NEDO) of Japan, and also by the Priority Assistance of the Formation of Worldwide Renowned Centers of Research – The 21st Century COE Program (Project: Center of Excellence for Advanced Structural and Functional Materials Design) from the Ministry of Education, Sports, Culture, Science and Technology of Japan.

References

[1] Shen P, Fujii H, Nogi K. Effect of crystallographic orientation on wettability and adhesion in several representative systems. In: Olabi Abdul-Ghani, Hashmi MSJ, editors. Proceedings of the International Conference on Advances in Materials and Processing Technologies, July 8–11, Dublin, Ireland; 2003. p. 1416.
[2] Champion JA, Keen BJ, Sillwood JM. J Mater Sci 1969;4:39.
[3] Mcevoy AJ, Williams RH, Higginbotham IG. J Mater Sci 1976;11:297.
[4] Weirauch Jr DA. J Mater Res 1988;3(4):729.
[5] Fujii H, Nakae H. ISIJ Inter 1990;30(12):1114.
[6] Nakae H, Fujii H, Sato K. Mater Trans JIM 1992;33(4):400.
[7] Yoshimi N, Nakae H, Fujii H. Mater Trans JIM 1990;31(2):141.
[8] Fujii H, Nakae H. Acta Mater 1996;44(9):3567.
[9] Nogi K, Tsujimoto M, Ogino K, Iwamoto N. Acta Metall Mater 1992;40(5):1045.
[10] Shen P, Fujii H, Matsumoto T, Nogi K. Scripta Mater 2003;48:779.
[11] Fujii H, Matsumoto T, Hata N, Nakano T, Kohno M, Nogi K. Metall Mater Trans A 2000;31:1586.
[12] Shen, P, Fujii, H, Matsumoto, T, Nogi K. J Am Ceram Soc [accepted].
[13] Henrich VE. Surf Sci 1976;57:385.
[14] Chern G, Huang JJ, Leung TC. J Vac Sci Technol A 1998;16(3):964.
[15] Joshi AB, Norton MG. Appl Surf Sci 1997;115:307.

[16] Plass R, Feller J, Gajdardziska-Josifovska M. Surf Sci 1998;414:26.
[17] Pojani A, Finocchi F, Goniakowski J, Noguera C. Surf Sci 1997;387:354.
[18] Plass R, Egan K, Collzao-Davila C, Grozea D, Landree E, Marks LD, Gajdardziska-Josifovska M. Phy Rev Lett 1998;81(2):4891.
[19] Okumiya M, Yama G. Bull Chem Soc Jpn 1971;44:1567.
[20] Stumpf HC, Russell Allen S, Newsome JW, Tucker CM. Ind Eng Chem 1950;42:1398.
[21] Aksay IA, Hoge CE, Pask JA. J Phys Chem 1974;78:1178.
[22] Eustathopoulos N. Acta Mater 1998;46(7):2319.
[23] Ito T, Kuramoto M, Yoshika M, Tokuda T. J Phys Chem 1983;87:4411.
[24] Kobayashi H, Yamaguchi M, Ito T. J Phys Chem 1990;94:7206.
[25] Kobayashi H, Salahub DR, Ito T. J Phys Chem 1994;98:5487.
[26] Sawabe K, Koga N, Morokuma K, Iwasawa Y. J Chem Phys 1992;97(9):6871.
[27] Shluger AL, Gale JD, Catlow CRA. J Phys Chem 1992;96:10389.
[28] Knözinger E, Jacob K-H, Singh S, Hofmann P. Surf Sci 1993;290:388.
[29] Knözinger E, Jacob K-H, Hofmann P. J Chem Soc Faraday Trans 1993;89(7):1101.
[30] Anchell JL, Morokuma K, Hess AC. J Chem Phys 1993;99(8):6004.
[31] Anchell JL, Glendening ED. J Phys Chem 1994;98:11582.
[32] Hermansson K, Baudin M, Ensing B, Alfredsson M, Wojcik M. J Chem Phys 1998;109(17):7515.
[33] Purton JA, Bird DM, Parker SC, Bullett DM. J Chem Phys 1999;110(16):8090.
[34] Goniakowski J, Noguera C. Phys Rev B 1999;60:16120.
[35] Goniakowski J, Noguera C. Phys Rev B 2002;66:085417.
[36] Benedek R, Minkoff M, Yang LH. Phys Rev B 1996;54:7697.
[37] Henrich VE, Cox PA. The surface science of metal oxides. Cambridge: Cambridge University Press; 1994.
[38] Tasker PW. Surface of magnesia and alumina. In: Kingry WD, editor. Structure and properties of MgO and Al_2O_3 ceramics. The American Ceramic Society; 1984. p. 176.
[39] Tasker PW, Duffy DM. Surf Sci 1984;137:91.
[40] Goniakowski J, Noguera C. Surf Sci 1995;323:129.
[41] Gibson A, Haydock R, LaFemina JP. J Vac Sci Technol A 1992;10(4):2361.
[42] Rohr F, Wirth K, Libuda J, Cappus D, Bäumer M, Freund H-J. Surf Sci 1994;315:L977.
[43] Hong T, Smith JR, Srolovitz DJ. Acta Metall Mater 1995;43(7):2721.
[44] Shen P, Fujii H, Matsumoto T, Nogi K. Acta Mater 2003;51(16):4897.
[45] Takeda H, Takeda M, Nogi K, Ogino K. Mater Trans JIM 1994;35(7):466.
[46] Refson K, Wogelius RA, Fraser DG, Payne MC, Lee MH, Milman V. Phys Rev B 1995;52:10823.
[47] Onishi H, Egawa C, Aruga T, Iwasawa Y. Surf Sci 1987;191:479.
[48] Almeida AL, Martins JBL, Longo E, Furtado NC, Taft CA, Sambrano JR, Lester Jr WA. Int J Quantum Chem 2001;84:705.